Title: Speciation and gene flow across an elevational gradient in New Guinea kingfishers

Running Title: Speciation in New Guinea kingfishers

Ethan Linck[1*], Benjamin G. Freeman[3], and John P. Dumbacher[4]

[1]*Department of Biology & Burke Museum of Natural History & Culture, University of Washington, Seattle, 98195, USA*

[2]*Department of Biology & Burke Museum of Natural History & Culture, University of Washington, Seattle, 98195, USA*

[3]*Beaty Biodiversity Research Centre, University of British Columbia, Vancouver, V6T 1Z4, CA*

[4]*Ornithology & Mammalogy, California Academy of Sciences, San Francisco, 94118, USA*

[*]Corresponding Author: ethanblinck@gmail.com

Abstract: Theory suggests speciation without geographic isolation is plausible if divergent natural selection is strong enough to counteract gene flow. Tropical mountains provide strong and temporally stable environmental gradients that can promote local adaptation and population genetic structure. Pairs of closely related species with adjacent but divergent elevational ranges are common in these environments, a pattern that suggests parapatric speciation (i.e., speciation with moderate gene flow), but evidence for this process is scarce. Here we use genomic data from modern and historical museum specimens to investigate speciation in a carefully chosen pair of sister New Guinea kingfisher species that segregate ranges by elevation. We find that the lowland species *Syma torotoro* and montane species *S. megarhyncha* form discrete genotypic clusters with bimodal variance in phenotypic traits. Phylogenetic relationships among lineages are discordant between mitochondrial and nuclear genomes, which *D*-tests and demographic inference indicate is partly driven by interspecific gene flow after an initial period of isolation. Summary statistics reveal differentiation is concentrated in a handful of small regions of the genome. These data underscore the apparent scarcity of convincing cases of parapatric speciation. However, they also suggest selection across elevational gradients can maintain species boundaries without strong intrinsic reproductive isolation, a mechanism contributing to high tropical biodiversity.

Key words: parapatric speciation, speciation genomics, ecological speciation, Syma

Introduction: Adaptation across environmental gradients is ubiquitous in nature (Turesson, 1925; McCormack & Smith, 2008; Cheviron & Brumfield, 2009), but its role in promoting speciation remains contentious (Coyne & Orr, 2004; Mallet, 2005; Fitzpatrick, Fordyce, & Gavrilets, 2008; Mallet, 2008). Disruptive natural selection can lead to local adaptation that restricts gene flow between populations in different environments if it becomes paired with a mechanism to promote nonrandom mating such as a pleiotropic "magic trait," linkage disequilibrium between separate loci involved with local adaptation and assortative mating, or habitat preference leading to ecogeographic isolation (Rundle & Nosil, 2005; Via, 2009; Nosil, 2012). A robust body of theory suggests this process is possible under a range of circumstances (Smith, 1966; Endler, 1977; Kirkpatrick & Ravigné, 2002; Doebeli & Dieckmann. 2003; Doebeli, Dieckmann, Metz, & Tautz, 2005; Hua, 2016). However, evolutionary biologists have traditionally dismissed its relevance in natural systems given the obvious efficiency of speciation without gene flow, and because there are few clear empirical examples (Coyne & Orr, 2004).

Tropical mountainsides generate strong and temporally stable environmental gradients, providing a useful setting for testing the role of local adaptation in generating species richness in nature. While allopatric divergence following dispersal or vicariance is doubtless an important factor in the origin of species in the tropics (Smith et al., 2014), the importance of abiotic and biotic ecological variables in driving evolutionary processes agnostic to geography is increasingly recognized (Polato et al., 2018). Ecologists have long known that reduced seasonal variation in temperature drives strong thermal stratification across tropical mountainsides (Polato et al., 2018; Janzen, 1967; Sheldon, Huey, Kaspari, & Sanders, 2018), a pattern correlated with high beta diversity (Jankowski, Ciecka, Meyer, & Rabenold, 2009; Cadena et al., 2012),

69 especially among closely related species (Terborgh & Weske, 1975; Freeman & Freeman, 2014).
70 Because many tropical taxa are residents that appear to show low rates of dispersal and have a
71 "slow pace of life" (Wiersma, Muñoz-Garcia, Walker, & Williams, 2007; Harvey, Aleixo, Ribas,
72 & Brumfield, 2017; Smith et al., 2017), strong disruptive selection could plausibly counteract the
73 homogenizing effects of gene flow to drive adaptive divergence.

74 Local adaptation across tropical elevational gradients has been documented by clines in
75 functional genes and intraspecific population genetic structure (Cheviron & Brumfield, 2009;
76 DuBay & Witt, 2014; Funk et al., 2016; Gadek et al., 2018). This has been shown theoretically to
77 "scale up" to speciation under a scenario of niche expansion (Hua, 2016), but empirical evidence
78 remains mixed. Phylogenetic and phylogeographic comparative studies suggest this process has
79 occurred in *Ithioma* butterflies (Elias et al., 2009) and Andean amphibians and reptiles (Arteaga
80 et al., 2016). In Andean birds, a broad consensus holds that elevational replacements primarily
81 form through divergence in allopatry followed by secondary contact and range displacement
82 (Cadena et al., 2012; DuBay & Witt, 2014; Caro, Caycedo-Rosales, Bowie, & Cadena, 2013;
83 Cadena & Céspedes, 2019), despite equivocal results in some tests. Yet we are aware of only one
84 study that has used population genomics to evaluate speciation across elevational gradients,
85 which found strong evidence that adaptation to altitude drives speciation in Senecio ragwort
86 plants in temperate Italy (Chapman, Hiscock, & Filatov, 2013; Osborne, Batstone, Hiscock, &
87 Filatov, 2013). The question of the relative contribution of adaptation in the presence of gene
88 flow across elevational gradients to speciation and broader patterns of tropical biodiversity
89 remains open.

90 The Yellow-billed and Mountain Kingfishers *Syma torotoro* and *S. megarhyncha* (Aves:
91 Alcedinidae) are putative sister taxa that segregate by elevation and vary only subtly in

92 phenotype (Mayr, 1942; Pratt & Beehler, 2015; Diamond, 1972). Several aspects of their
93 distribution and ecology make the pair unusually plausible candidates for speciation driven by
94 divergent natural selection in the absence of significant geographic isolation (Rand, 1936). First,
95 *S. megarhyncha* is only found in the highlands of New Guinea, where it replaces *S. torotoro*
96 above ~1000 m throughout most of the island (Pratt & Beehler, 2015). A scenario of divergence
97 in allopatry is therefore less parsimonious than divergence in parapatry, as it requires substantial
98 historical range shifts. Second, in the Arfak and Tamrau mountains of western New Guinea
99 where *S. megarhyncha* is absent, *S. torotoro* does not expand its elevational range upslope,
100 suggesting the two species are not partitioning a shared fundamental niche (Beehler & Pratt,
101 2016). This hypothesis is strengthened by evidence of morphological adaptation to a cooler
102 climate in the larger-bodied *S. megarhyncha* (Beehler & Pratt, 2016). Third, *Syma* are territorial
103 and sedentary, making it plausible that dispersal was sufficiently reduced to be overcome by
104 divergent selection across the steep environmental gradient they inhabit (Endler, 1977).
105 However, species limits and range-wide variation have never been quantitatively assessed and
106 observed differences might instead reflect phenotypic plasticity or clinal variation of a single
107 widespread lineage (Caro et al., 2013).
108 Here we use genome-wide DNA sequences, bioacoustic data, and morphometric analyses
109 to investigate processes of speciation in *Syma* kingfishers. We assessed species limits and
110 phylogenetic relationships, tested for introgression and inferred demographic history, and
111 described the landscape of genomic divergence. If speciation was driven by local adaptation in
112 the absence of geographic isolation, we expected *S. torotoro* and *S. megarhyncha* to be
113 reciprocally monophyletic taxa showing evidence of gene flow throughout their history of
114 divergence. If speciation occurred in allopatry followed by range expansion and elevational

displacement, we expected to see little evidence of past or present gene flow, as this scenario would require sufficient reproductive isolation to develop to permit coexistence without genetic homogenization and the fusion of lineages on secondary contact. If speciation occurred in allopatric driven by adaptation to altitude and subsequent habitat isolation but few postzygotic barriers, we expected to see support for a model of secondary contact and evidence of recent gene flow.

Materials and Methods: *Study system.* Yellow-billed Kingfisher *Syma torotoro* and Mountain Kingfisher *Syma megarhyncha* (Aves: Alcedinidae) are the sole members of their genus. Members of the tree kingfisher subfamily Halcyoninae, they are endemic to New Guinea, its satellite islands, and the Cape York Peninsula of Australia. *S. torotoro* is found in tropical lowland forest and savannah from sea level to ~500 m elevation, or less commonly to ~1100 m (Pratt & Beehler, 2015). *S. megarhyncha* is found from ~600 m to 2700 m or higher (Pratt & Beehler, 2015). Though cited as a classic example of congeneric elevational replacements occurring in parapatry (Diamond, 1972), their elevational ranges have also been reported to either overlap (Gregory, 2017) or be separated by a substantial gap (Freeman & Freeman, 2014; Sam, Koane, & Novotny, 2014). Both species are omnivorous territorial interior forest residents and differ only in *S. megarhyncha's* larger body size, deeper call, and the extent of black on the top of its bill in one subspecies (Pratt & Beehler, 2015). Insular *S. torotoro* subspecies *S. t. ochracea* differs substantially from its conspecifics and *S. megarhyncha* in call, and is intermediate in size, leading some authors to propose it represents a distinct species (Beehler & Pratt, 2016).

137 *Morphological and bioacoustics data.* We measured bill length, bill depth, tarsus, wing
138 chord, and tail length from 72 museum specimens of *Syma torotoro (n*=40) and *S. megarhyncha*
139 (*n*=32) at the American Museum of Natural History, collected from 1894-1965 and including
140 only individuals of known sex as originally identified by the preparator. Using these data, we
141 performed principal component analyses in R (R Core Team 2018) with normalized variables
142 and used PC1 to build mixture models using the R package mclust v. 5.4.1, which we evaluated
143 with a maximum likelihood classification approach (Scrucca, Fop, Murphy, & Rafferty, 2016).
144 We downloaded all available vocalizations from *S. torotoro* (*n*=34) and *S. megarhyncha* (*n*=14)
145 from xeno-canto and Cornell's Macaulay Library. We filtered these data for quality and
146 quantified 36 standard bioacoustic variables using the warbleR package v. 1.1.14 in R (Araya-
147 Salas & Smith-Vidaurre, 2017), analyzing 278 distinct vocalizations from *S. torotoro* and 106
148 from *S. megarhyncha* in total. We ran PCA with normalized variables on the output and used
149 these data to alternate species delimitation models using the same approach as with our
150 morphological data.
151 *Sampling, library preparation, and DNA sequencing.* We extracted DNA from fresh
152 tissues (*n*=6) and toepad samples from historical museum specimens (*n*=34) from 30 individuals
153 of *S. torotoro* (*n*=30) and 10 individuals of *S. megarhyncha* (*n*=10). Though only partially
154 overlapping with samples used in morphometric analyses, these individuals represented the full
155 extent of both species' ranges in New Guinea and Australia (Table 1) and included all described
156 subspecies. We extracted DNA from fresh tissues using a Qiagen DNAeasy kit and the
157 manufacturer's recommended protocol. For historical toepad samples (collected 1877-1973), we
158 extracted DNA using either a using a phenol-chloroform and centrifugal dialysis method
159 (Dumbacher & Fleischer, 2001) (for reduced representation sequencing) or a standard salt

160 extraction protocol (for whole genome sequencing). Due to constraints of cost and time, we
161 employed two complementary sequencing approaches. On a subset of samples (*n*=20), we
162 performed reduced representation genome sequencing using a hybridization capture with RAD
163 probes (hyRAD) approach, described in detail elsewhere (Linck, Hanna, Sellas, & Dumbacher,
164 2017). We sent the remaining samples to the UC Berkeley's Vincent J. Coates Genomic
165 Sequencing Laboratory, where laboratory staff prepared genomic libraries for low coverage
166 whole genome sequencing (WGS) using Illumina TruSeq Nano kits and a modified protocol that
167 skipped sonication and enzymatically repaired fragments with RNAse. They then pooled (*n*=20)
168 and sequenced these samples with 150 base pair paired end reads on a single lane of an Illumina
169 HiSeq 4000.

170 *Sequence assembly and variant calling.* We processed demultiplexed reads from both
171 sequencing strategies together with a custom bioinformatic pipeline optimized for handling
172 degraded DNA data and available at https://github.com/elinck/syma_speciation. Briefly, we
173 trimmed raw reads for adapters and low-quality bases using bbduk from BBTools version 38.06
174 suite of bioinformatics tools. We aligned these reads to an unpublished draft genome of
175 Woodland Kingfisher *Halcyon senegalensis* from the Bird 10K Genome Project using bbmap
176 with a k-mer value of 12, a maximum indel length of 200 bp, and a minimum sequence identity
177 of 0.65. These highly sensitive alignment parameters were necessary given the clade containing
178 Syma diverged from the clade containing *Halcyon* approximately 15 mya (Andersen,
179 McCullough, Mauck, Smith, & Moyle, 2018). We used PicardTools v. 2.17.8 and GATK v. 3.6.0
180 (McKenna et al., 2010) to append read groups and perform local realignment on .bam files. We
181 then used mapDamage 2.0.9 to account for postmortem damage to DNA from historical museum
182 specimens by rescaling quality scores (Jónsson, Ginolhac, Schubert, Johnson, & Orlando, 2013).

183 We performed multisample variant calling using the UnifiedGenotyper tool in GATK v. 3.6.0,
184 and filtered our variant calls for missing data, coverage, and quality with VCFtools 0.1.16
185 (Danecek et al., 2011). We generated multiple SNP datasets by implementing different filters to
186 suit the requirements and goals of different analyses; these settings and their underlying rationale
187 are described in detail below. To complement our nuclear DNA sequences, we assembled near-
188 complete and fully annotated mitochondrial genomes from a majority of individuals using
189 mitofinder v. 1.0.2 and a complete mtDNA genome from close relative *Todiramphus sanctus* as
190 a reference (Andersen et al., 2015). We then extracted NADH dehydrogenase 2 (ND2) from
191 these genomes and performed multiple sequence alignment using MAFFT v7.407 under its "–
192 auto" parameter setting package (Katoh & Standley, 2013).

193 *Population structure inference.* We evaluated population genetic structure within and
194 between species using a nonparametric clustering approach. We performed principal component
195 analysis of genotypes (PCA) and identified putative genetic clusters for K=2 through K=4 using
196 adegenet v. 2.1.1 (Jombart, 2008) and a 95% complete dataset with 66,917 SNPs from all
197 individuals in both datasets with a minimum depth of coverage of 3x per individual, a maximum
198 depth of coverage of 120x per individual, a minimum quality score of 30, and a minimum minor
199 allele frequency of 0.05. These relatively lenient filtering parameters were chosen to permit the
200 inclusion of samples from both sequencing strategies in our initial assessment of probable
201 species limits. We evaluated the best-fit clustering model using the Bayesian Information
202 Criterion, again implemented in adegenet.

203 *Phylogenetic inference.* We evaluated phylogenetic relationships among lineages with
204 three complementary approaches. Using our mitochondrial DNA (ND2) alignment, we inferred a
205 time-calibrated phylogeny in BEAST 2.6.0 (Bouckaert et al., 2019) including all samples and

206 Sacred Kingfisher *Todiramphus sanctus* as an outgroup (Andersen et al., 2015). We used a strict
207 molecular clock with a rate of 2.9×10^{-8} following Lerner, Meyer, James, Hofreiter, & Fleischer
208 (2011), a GTR+GAMMA model of nucleotide evolution, and a Yule species tree prior. We ran
209 BEAST for 50 million generations, storing trees every 1000 generations, and assessed mixing,
210 likelihood stationarity and adequate effective sample sizes (ESS) above 200 for all estimated
211 parameters using Tracer v.1.7.1 (Rambaut, Drummond, Xie, Baele, & Suchard, 2018). We then
212 generated a maximum clade credibility tree using TreeAnotator v.2.6.0, discarding the first 10%
213 of trees as burnin (Bouckaert et al., 2019). We next inferred a nuclear DNA phylogeny using
214 SVDquartets (as implemented in PAUP v.4.a165) without *a priori* species assignments
215 (Chiffman & Kubatko, 2014). To reduce the influence of sequencing errors, we used a
216 stringently filtered SNP dataset, including only whole genome sequencing data, sites with a
217 minimum minor allele count of 3, no more than 10% missing data, a minimum depth of 5x and a
218 maximum depth of 120x per individual, and a minimum quality score of 30. We converted this
219 diploid alignment to a single consensus IUPAC ambiguity code per individual using vcf2phylip
220 v2.0 (Ortiz, 2019) and included the reference sequence from *H. senegalensis* as an outgroup. We
221 ran SVDquartets with 2000 quartets and 100 bootstrap replicates. Lastly, we inferred a species
222 tree under a multispecies coalescent model with SVDquartets and the same SNP dataset as
223 above, using taxon partitions concordant with k-means clustering results and ND2 lineages and
224 the speciesTree=Yes parameter setting.
225 *Demographic inference*. We inferred the demographic history of diverging lineages using
226 moments v.1.0.0, which uses ordinary differential equations to model the evolution of allele
227 frequencies (Jouganous, Long, Ragsdale, & Gravel, 2017). We used the joint_sfs_folded()
228 function in Python package scikit-allel v.1.2.1 (Miles, Ralph, Rae, & Pisupati, 2019) to calculate

229 a folded joint site frequency spectrum (JSFS) using a SNP dataset that included only whole
230 genome sequencing data, a minimum minor allele count of 1, no more than 10% missing data per
231 site, a minimum depth of 6x per individual, and a minimum quality score of 30. We chose these
232 filtering parameters to reduce the influence of sequencing error without strongly biasing the
233 JSFS. This dataset did not include *S. t. ochracea,* and had been further thinned to include only
234 variants in approximate linkage equilibrium (defined as sites where $r^2<0.1$) using scikit-allel's
235 locate_unlinked() function. To account for the remaining missing data, we projected the JSFS
236 down to an effective sample size of 16 x 12 chromosomes for *S. megarhyncha* and *S. torotoro*
237 respectively.

238 We then specified four basic demographic models chosen to represent plausible
239 speciation scenarios in *Syma,* which differed by level and timing of gene flow. These were: an
240 isolation-with-migration model (IM), which permitted gene flow throughout the history of
241 diverging lineages; an isolation-with-ancestral-migration model (AM), which featured an initial
242 period of gene flow followed by a period of isolation; a model of secondary contact (SC), which
243 featured an initial period of isolation followed by a period of gene flow; and a model of strict
244 isolation (SI), which allowed no gene flow following initial divergence. Next, we specified four
245 additional models which differed from each of the above only by allowing exponential
246 population growth in the most recent time period: an isolation-with-migration-and-growth model
247 (IMg), an isolation-with-ancestral-migration-and-growth model (AMg), a secondary contact and
248 growth model (SCg), and a strict isolation and growth model (SIg).

249 After initially optimizing parameters for fitting each model using the "optimize log"
250 method and a maximum of 3 iterations, we ran 9 additional optimizations, randomly sampling
251 starting values from a uniform distribution within the bounds of $1x10^{-4}$ and 10. We converted

252 parameter values to real units using a genome-wide mutation rate of 2.3×10^{-9} (Smeds,
253 Qvarnström, & Ellegren, 2016), an effective sequence length scaled to reflect our LD-thinned
254 SNP dataset, and a generation time estimate of two years. We generated parameter uncertainty
255 estimates for the best-fit demographic model (selected based on AIC values) by fitting it to 200
256 bootstrapped site frequency spectra generated using the fs.sample() function on our data, an
257 approach which is appropriate when sites are unlinked (Jouganous et al., 2017).

258 *Introgression.* We explicitly tested for introgression between lineages using the four
259 taxon *D*-test (Green et al., 2010), which relies on asymmetries in discordant site patterns to
260 distinguish incomplete lineage sorting from introgression. We randomly selected one
261 representative sequence for *S. torotoro*, *S. megarhyncha*, and *S. t. ochracea* from the nuclear
262 DNA SNP alignment used in our phylogenetic analyses, and again used the reference sequence
263 for *H. senegalensis* as an outgroup. We then calculated *D* using a custom python script (available
264 at https://github.com/elinck/syma_speciation/), estimating uncertainty using a block jacknife
265 with 100 replicates.

266 *Genome scans.* We assessed levels of divergence across the genome by calculating
267 Wright's F_{ST} and D_{XY} in 50 kbp windows with a 10 kbp step size using scripts written by Simon
268 Martin (https://github.com/simonhmartin/genomics_general), using a VCF file generated from
269 our whole genome sequencing data that included invariant sites and was filtered for a minimum
270 Q score of 30 and a minimum depth of 3x per individual, for a total of 1,858,764 SNPs and
271 102,606,487 total sites. We permitted a lower depth of coverage threshold in this analysis as our
272 goal was to describe the overall landscape of differentiation as completely as possible given the
273 constraints of our data. To assign chromosome identity to scaffolds and windows, we aligned the
274 *H. senegalensis* draft genome to the chromosome-level genome assembly of *Taenopygia guttata*

275 (Warren et al 2010) using NUCmer in MUMmer v. 3.1 (Delcher et al., 1999), allowing a
276 maximum gap of 1000 bp and using a minimum sequence identity threshold of 10 kbp per
277 contig. We evaluated correlations among summary statistics using simple linear models
278 implemented in R (R Core Team, 2018).
279
280 **Results:** *DNA sequencing from historical specimens.* We extracted DNA and generated
281 genome-wide sequence data from all historic toepad samples across both species' relatively
282 inaccessible distributions, with collection dates ranging from 1896 to 1973 and including 3
283 individuals collected by Ernst Mayr himself in 1929. We present a detailed description of
284 reduced representation hyRAD data elsewhere (Linck et al., 2017). On average we were able to
285 align 83.3% of reads to the draft *Halcyon senegalensis* genome, ranging from 35.5% to 92.37%
286 across individuals; this broad range likely reflects high DNA degradation in a handful of
287 samples. Whole genome sequencing data had an average depth of coverage of 5.38x per
288 individual, ranging from 1.92x to 12.12x. Following variant calling and filtering for depth of
289 coverage and quality, a 95% complete data matrix including 37 individuals and both WGS and
290 hyRAD data had 66,917 SNPs, which was further reduced to 10,351 SNPs after thinning to 1 site
291 for every 50 kbp to reduce the influence of linkage disequilibrium. A second matrix of whole
292 genome sequencing data alone had 78,882,912 SNPs, which was reduced to 1,858,764 SNPs
293 after filtering for a minimum depth of coverage of 3x and a minimum quality score of 30.
294 *Species limits and phylogeny.* Analysis of genome-wide DNA sequence data,
295 morphometrics, and calls supported *Syma torotoro* and *S. megarhyncha* as distinct, assortatively
296 mating lineages (Figure 1). Principal component analysis of genotypes separated *S. torotoro* and
297 *S. megarhyncha* into discrete clusters (Figure 1A; Figure 1C) with little evidence of hybrid

genotypes along the primary axis of genetic differentiation, with PC1 explaining 17.02% of total variance. PC2 explained 6.31% of total variance and separated insular subspecies *S. t. ochracea* into a third discrete cluster. The best-fit model from a k-means clustering analysis (as identified by BIC scores) perfectly recovered these groups (Figure 1C).

Analyses of phenotypic data formed discrete clusters concordant with genomic results and consistent with morphological differentiation by elevation. Bill width and depth, tarsus, wing chord, and tail length were significantly larger in *Syma megarhyncha* after correcting for multiple comparisons in Welch's two sample T-tests (all comparisons $p<1x10^{-7}$), and species was a significant predictor of PC1 in a linear model ($p<1x10^{-14}$). Following principal component analysis, PC1 explained 81.47% of variance across all five traits. Bayesian Information Criterion (BIC) selected two distinct normal distributions out of normal mixture models (NMMs) fit to PC1 (log-likelihood=−378.0914) (Figure 1D). Calls of *S. torotoro* had a significantly higher frequency ($p<1x10^{-5}$) but did not differ in duration. Species was a significant predictor ($p<1x10^{-5}$) of PC1 in a principal component analysis of the 36 bioacoustic variables quantified in warbleR (Araya-Salas & Smith-Vidaurre, 2017) and explained 35.72% of total variance. Because NMMs assume independence of observations, we did not perform formal model fitting for bioacoustic data, but a frequency distribution strongly suggests values are bimodally distributed by species identity (Figure 1E).

A time-calibrated phylogeny of the mitochondrial gene ND2 supported the reciprocal monophyly of *S. megarhyncha* and *S. torotoro,* but unexpectedly recovered mainland *S. torotoro* as sister with a clade containing *S. megarhyncha* and insular endemic subspecies *S. t. ochracea* (Figure 1F). Within *S. torotoro,* a clade of four individuals with full bootstrap support from the southeast peninsula of Papua New Guinea was separated from the remaining individuals, but

321 with little other apparent geographic structure across the tree. Based on a strict molecular clock
322 with a rate of 2.9x10−8, *S. megarhyncha* and *S. t. ochracea* initially diverged from *S. torotoro*
323 approximately 790,000 years ago (95% CI: 607,422-972,619 years); a subsequent split between
324 *S. megarhyncha* and *S. t. ochracea* occured approximately 377,997 years ago (95% CI: 243,262-
325 512,732 years), and a split between *S. torotoro* populations in the SE peninsula of Papua New
326 Guinea and the rest of the species occurred approximately 428,580 years ago (95% CI: 304,805-
327 552,355 years). In contrast, our nuclear DNA lineage phylogeny was more poorly resolved and
328 conflicted with both the ND2 tree and current taxonomy (Figure 1G). An initial divergence event
329 with full bootstrap support separated a clade containing *S. megarhyncha* individuals from far
330 western New Guinea and *S. t. ochracea*; a second fully supported split separated S. torotoro
331 populations in SE Papua New Guinea from an ingroup containing poorly resolved clades
332 containing the remainder of *S. torotoro* and *S. megarhyncha* individuals. Lastly (and again
333 conflicting with both other phylogenies), our nuclear DNA species tree from SVDquartets
334 grouped *S. torotoro* and *S. megarhyncha* together in a clade that was sister to *S. t. ochracea*, with
335 full bootstrap support at all internal nodes (Figure 1H)
336 *Demographic history and introgression. D*-tests indicated asymmetric genealogies among
337 lineages that were the product of introgression or ancestral population structure rather than
338 incomplete lineage sorting alone. For two of three possible species tree topologies, *D* differed
339 signficantly from 0 (one sample t-tests: $p<2x10^{-16}$ and t=877.23 given
340 (ochracea,megarhyncha),torororo); $p<2x10^{-16}$ and t=837.36 given
341 (ochracea,torotoro),megarhyncha)), with signs indicating introgression between *S. torotoro* and
342 *S. megarhyncha*, rather than either of these species and *S. t. ochracea* (Figure 1A). Bootstrapped
343 *D*-test values for the topology (megarhyncha,torororo),ochracea) also different significantly from

344 zero (one sample t-test: $p<2x10^{-16}$ and $t=-19.416$), but with a range which encompassed it (-
345 0.023 to 0.003).

346 The best-fit demographic model involved secondary contact without recent exponential
347 population growth (AIC=1140.124; log-likelihood=-564.062), followed by a model of ancestral
348 migration (AIC=1192.047; log-likelihood=-590.062) (Table 2). Parameter estimates from the
349 secondary contact model provide additional evidence for introgression and suggest it has been
350 ongoing for long time periods (Figure 2B, 2C, 2D). After an initial period of approximately
351 458,469 years of geographic isolation following divergence (SD: 6,162 years), we inferred *Syma*
352 species have been exchanging genes for ~191,231 years (SD: 7,510 years) at a rate of 1.14
353 individuals per generation (SD: 0.023) from *S. torotoro* to *S. megarhyncha*, and a rate of 0.12
354 individuals per generation (SD: 0.006) from *S. megarhyncha* to *S. torotoro.* Summing the first
355 and second periods indicates an initial divergence event approximately 649,700 years ago—a
356 date consistent with the estimate from the mitochondrial DNA molecular clock analysis. We
357 inferred a population size for *S. torotoro* of ~1,909,985 individuals (SD: 26,028) and a
358 population size for *S. megarhyncha* of ~368,390 individuals (SD: 8,528).

359 *Genome scans.* Analysis of whole genome sequencing data suggests *S. torotoro* and S.
360 megarhyncha differ primarily in small regions of the genome (Figure 3A). Genome scans of
361 divergence in 50 kb sliding windows with a step size of 10 kb revealed globally low to moderate
362 genetic divergence (mean F_{ST}=0.0947) defined by 21 autosomal F_{ST} peaks (Figure 3A; Figure
363 3B). The Z chromosome showed low interspecific divergence, suggesting a limited role in
364 speciation (Irwin, 2018), though this may represent an artifact of high intraspecific diversity due
365 to misincorporation of reads from the W chromosome. Correlations between genome-wide
366 summary statistics suggested a role for both structural reductions in recombination and positive

367 selection in shaping F_{ST} peaks. F_{ST} was negatively but weakly correlated with D_{XY} ($p<1x10^{-15}$,
368 R^2=0.1271) (Figure 3A). Considering a subset of chromosomes with prominent F_{ST} peaks (Figure
369 3B), this correlation remained significant but was slightly reduced ($p<1x10^{-15}$, R^2=0.1044)
370 (Figure 3C).
371
372 **Discussion:** Speciation across environmental gradients is commonly invoked in
373 explanations of high tropical species richness and the latitudinal biodiversity gradient (Caro et
374 al., 2013; Schneider, Smith, Larison, & Moritz, 1999; Portik et al., 2017; Beheregaray, Cooke,
375 Chao, & Landguth, 2015). Tropical elevational gradients have high levels of temporally stable
376 thermal stratification (Janzen, 1967) that has been linked to selection for narrow thermal
377 physiologies (Sheldon et al., 2018), reduced upslope or downslope dispersal (Polato et al., 2018),
378 and high beta diversity (Jankowski et al., 2009). As a result, they have frequently been studied as
379 a stage for this process (Mayr, 1942; Cadena et al., 2012; Funk et al., 2016; Arteaga et al., 2016;
380 Caro et al., 2013; Moyle, Manthey, Hosner, Rahman, Lakim, & Sheldon, 2017). Yet previous
381 comparative phylogenetic studies have overwhelmingly supported models of divergence in
382 allopatry followed by secondary contact and range displacement without gene flow, particularly
383 in vertebrates (Arteaga et al., 2016; Caro et al., 2013; Moyle et al., 2017). Our finding of well-
384 defined genotypic and phenotypic clusters (Figure 1) in the face of recent introgression (Figure
385 2) suggests that selection across elevational gradients is sufficient to maintain species boundaries
386 with little evidence of strong postzygotic isolation. This result supports an intuitive and widely
387 cited but poorly buttressed theory: that selection across environmental gradients can serve as a
388 motor for tropical diversification, either as the primary driver of speciation (e.g., in ecological

389 speciation models) or as a force for reinforcement and disruptive selection after the build-up of
390 partial reproductive isolation in allopatry.

391 Though evidence from genotypic and phenotypic clustering analyses suggests *S. torotoro*
392 and *S. megarhyncha* are assortatively mating lineages that are largely match current taxonomy,
393 alternate approaches to phylogenetic inference provide conflicting data on species limits and
394 evolutionary relationships. A well-sampled phylogeny of the mitochondrial gene ND2 shows an
395 unexpected sister relationship between *S. megarhyncha* and insular *S. torotoro* subspecies
396 ochracea, previously hypothesized to represent a species-level lineage (Pratt & Beehler, 2015),
397 but also revealed the expected pattern of monophyly for *S. torotoro* and *S. megarhyncha*. In
398 contrast, a phylogeny from nuclear DNA is strongly discordant with both mitochondrial
399 relationships and the results of clustering analyses (Figure 1E). We propose this conflict can be
400 primarily explained by introgression between *S. torotoro* and *S. megarhyncha* in eastern New
401 Guinea, as supported by evidence from *D*-tests and demographic inference (Figure 2). Increased
402 structure in mitochondrial DNA relative to the nuclear genome may also be generated by with
403 reduced hybrid fitness in heterogametic females (in accordance with Haldane's rule), or male
404 biased dispersal (Toews & Brelsford, 2012)—both of which are plausibly contributing to
405 patterns in *Syma*.

406 Despite this phylogenetic uncertainty, we believe our data from *Syma* are consistent with
407 speciation with driven by niche expansion and disruptive selection across an elevational gradient
408 in allopatry followed by secondary contact and recent gene flow. Divergence in morphometric
409 traits, the most visible phenotypic difference between *S. torotoro* and *S. megarhyncha* (Figures
410 1D, 1E), is largely thought to reflect ecological adaptation in allopatric populations (Ricklefs &
411 Bermingham, 2007; Winger & Bates, 2015). While this may arise as a result of character

412 displacement from competition in populations experiencing secondary contact (Diamond, Pimm,
413 Gilpin, & LeCroy, 1989), it presumes sufficient reproductive isolation has developed to permit
414 coexistence without genetic homogenization and the fusion of lineages. In *Syma*, tests for
415 introgression and demographic inference indicate gene flow has occurred for nearly 200,000
416 years, rendering the presence of strong genetic incompatibilities unlikely. Though we cannot rule
417 out a role for ancestral population structure in generating significant *D*-test results, parameter
418 estimates from our best fit demographic model and reports of occasional hybridization in the
419 field (Beehler & Pratt, 2016) provide additional evidence for introgression. Additionally, the
420 failure of *S. torotoro* to expand its elevational range upslope in absence of *S. megarhyncha* in the
421 mountains of the Vogelkop Peninsula in West Papua supports a hypothesis of adaptation to
422 divergent elevational niches, rather than competitive segregation of a shared, broader realized
423 niche.

424 However, we emphasize that in conflict with distributional, ecological, and
425 morphological evidence, our genomic data fail to support a traditional model of parapatric
426 speciation—or what Endler (1977) termed "primary" intergradation. Given *Syma* appeared to be
427 an unusually plausible candidate for this process, our results underscore the apparent rarity of the
428 phenomenon in nature. While this is no doubt partly due to the stronger divergent selection
429 required to achieve the evolution of reproductive isolation in the face of gene flow compared to
430 in allopatry, we suggest the geographic complexity of landscapes and stochastic population size
431 changes overtime are additional factors rendering truly parapatric divergence unlikely. There is
432 some evidence that even the contemporary distribution of *Syma* is less continuous than it is
433 typically described: recent surveys on Mt. Wilhelm and Mt. Karimui in Papua New Guinea
434 found large gaps in the elevational ranges of *S. torotoro* and *S. megarhyncha* (Freeman &

435 Freeman, 2014; Sam et al., 2014), in contrast to earlier studies (Diamond, 1972). It is therefore
436 easy to imagine orogenic vicariance or a dispersal event into the highlands from the common
437 ancestor of *S. torotoro* and *S. megarhyncha* might have resulted in a substantial period of
438 geographic isolation despite relatively short horizontal distances between species' ranges.

439 Though we did not identify the targets of selection, our data are consistent with disruptive
440 positive selection leading to high divergence in small regions of the genome against a
441 background of long-term introgression. These genomic "islands" have become a hallmark of the
442 high throughput sequencing era and have been shown in wide range of nonmodel organisms
443 (Nosil, 2012; Bay & Ruegg 2017). Early interpretations of the pattern as a clear signature of
444 speciation with gene flow—where F_{ST} peaks correlate to genes for traits under disruptive
445 selection while low F_{ST} regions remain susceptible to introgression—have been complicated by
446 evidence numerous processes can produce similar distributions, including selective sweeps in
447 allopatry or linked selection paired with recombination rate variation (Cruickshank & Hahn,
448 2014; Bay & Ruegg 2017; Irwin et al., 2018; Via, 2012; Burri, 2017). Evidence from multiple
449 summary statistics across the same genomic windows can also help tease apart underlying
450 mechanisms in some cases (Irwin et al., 2018): for instance, low absolute differentiation (D_{XY}) in
451 genomic islands can indicate F_{ST} values are inflated by low intraspecific diversity, casting doubt
452 on models of divergence with gene flow (Cruickshank & Hahn, 2014).

453 Here, our data defy easy description, highlighting the limits of this approach. A handful
454 of major F_{ST} peaks stand out against a background of low F_{ST} windows, with a global average of
455 0.0947 (Figure 3A; Figure 3B). However, D_{XY} shows only a weak correlation with *FST* values
456 (Figure 3C), which is further reduced in outlier windows. Low in some F_{ST} peaks and high in
457 others, this relationship supports the likely hypothesis that recombination rate, selection against

458 hybrid ancestry, disruptive selection, and gene flow have interacted to form a complex mosaic in
459 the genomes of *S. torotoro* and *S. megarhyncha.* Given the limitations of short-read sequencing
460 data, however, we concede these patterns may be influenced by either alignment artifacts or
461 undetected structural rearrangements. In particular, we point to large peaks on chromosomes 5
462 and 11 that deserve further scrutiny as possible inversions contributing to reproductive isolation
463 (Hooper & Price, 2017) (Figure 3A and 3B).

464 As adaptive differentiation in morphology appears to have occurred during the initial
465 stages of lineage divergence, *Syma* is plausibly a case of ecological speciation *sensu* Nosil and
466 Schluter (Rundle & Nosil, 2005; Nosil, 2012; Schluter, 2009), who define the process agnostic to
467 the presence or absence of gene flow. While we lack strong evidence for a target of disruptive
468 selection or a specific mechanism to link it to reproductive isolation, we speculate selection on
469 body size may also affect mate choice. Morphometric data from *Syma* are consistent with
470 Bergmann's rule and its prediction of larger body size in the higher elevation cooler climate
471 species, *S. megarhyncha* (but see Freeman (2017)). As one of only three kingfisher species found
472 above 2000 m in New Guinea and the only regional kingfisher that is a high elevation specialist,
473 *Syma megarhyncha* is likely to have a thermal physiology under stronger selective constraint for
474 warm environments, requiring greater adaptive divergence in body size to colonize montane
475 environments. An increase in body size might directly lower frequency calls as a biproduct of
476 morphological divergence, and assortative mating might act on either trait individually or in
477 tandem (Derryberry et al., 2018; Slabbekoorn & Smith, 2002; Zhen et al., 2017).

478 What does *Syma* reveal about the origin of elevational series of congeners and by
479 extension their significant contribution to tropical montane biodiversity (Freeman & Freeman,
480 2014)? First, our results suggest disruptive selection across elevational gradients can effectively

maintain species limits in the absence of strong postzygotic reproductive isolation, a finding with broad relevance to speciation in tropical mountains regardless of the geographic mode of divergence or levels of gene flow. In a scenario of secondary contact without adaptation to divergent elevational niches, *Syma* lineages would likely have fused. This suggests allopatric divergence may not be sufficient in isolation of other processes to drive many speciation events in tropical mountains and highlights the important role of habitat isolation in speciation processes in taxa (like birds) that are slow to evolve reproductive incompatibilities. Yet at the same time, our failure to find evidence for parapatric speciation in *Syma* in spite of its apparent plausibility make the process seem likely to be vanishingly rare in birds, at least across tropical elevation gradients. Furthermore, while New Guinea is large and geologically complex, it is dwarfed by other tropical montane regions, which potentially have increased odds for speciation in allopatry (Pratt & Beehler, 2015; Price, 2008). Still, we emphasize even if speciation across elevational gradients remain a rare exception among birds, the conditions that make it possible in *Syma* are more common in other taxa. Indeed, preliminary studies suggest it may be a much more common mechanism in amphibians, insects, and plants (Funk et al., 2016; Elias et al., 2009; Arteaga et al., 2016; Chapman et al., 2013). We highlight the importance of natural history studies of poorly known tropical organisms in establishing candidates for further investigation with genomic and experimental approaches.

Data availability: All code used in this study can be found at https://github.com/elinck/syma_speciation Processed data are available from Dryad [doi: pending], and sequence data are available from the NCBI SRA [accession: pending].

Acknowledgements: We thank generations of New Guinean landowners and field assistants without whose help this paper would have been impossible to write. For tissue loans, we thank L. Josef at ANWC, K. Zykowski at YPM, R. Moyle and M. Robbins at KUMNH, P. Sweet at AMNH, and R. Prys-Jones at NHMUK-Tring. For help arranging fieldwork, we thank A. Mack, G. Kapui, J. Robbins, N. Gowep, B. Beehler, L. Dabek, N. Whitmore, F. Dem, S. Tulai, B. Iova., and V. Novotny. We thank A. Wiebe for assistance measuring specimens and thank C.J. Battey for his many contributions. We additionally thank Y. Brandvain and three anonymous reviewers for their invaluable feedback. This work was supported by NSF Doctoral Dissertation Improvement Grant #1701224 to J. Klicka and E.B.L, a NDSEG Fellowship to E.B.L., and by NSF DEB #0108247 to J.P.D.

514 **Table 1.** Sampling, sequencing, and analysis information. WP=Indonesian New Guinea; PNG=Papua New Guinea.
515

Specimen	Species	Subspecies	Locality	Tissue source	Date collected	Sequencing strategy	PCA	mtDNA phylogeny	nuDNA phylogeny	D-tests	Demographic inference	Genome scans
AMNH:Birds:293714	torotoro	torotoro	Ifaar, WP	toepad	1928	hyRAD	yes	yes	no	no	no	no
AMNH:Birds:293715	torotoro	torotoro	Kepaur, WP	toepad	1897	hyRAD	yes	yes	no	no	no	no
AMNH:Birds:300723	torotoro	torotoro	Kepaur, WP	toepad	1897	hyRAD	yes	yes	no	no	no	no
AMNH:Birds:300723	torotoro	torotoro	Misol Island, WP	toepad	1900	hyRAD	yes	yes	no	no	no	no
AMNH:Birds:329542	torotoro	torotoro	Wasior, WP	toepad	1928	hyRAD	yes	yes	no	no	no	no
AMNH:Birds:437798	torotoro	torotoro	Amberbaki, WP	toepad	1877	hyRAD	yes	yes	no	no	no	no
AMNH:Birds:637429	torotoro	torotoro	Humbolt Bay, WP	toepad	1928	hyRAD	yes	yes	no	no	no	no
AMNH:Birds:637441	torotoro	torotoro	Mt. Mori, WP	toepad	1899	hyRAD	yes	yes	no	no	no	no
AMNH:Birds:637445	torotoro	torotoro	East Sepik Province, PNG	toepad	2003	hyRAD	yes	yes	no	no	no	no
AMNH:Birds:637446	torotoro	torotoro	Waigeu Island, WP	toepad	1900	hyRAD	yes	yes	no	no	no	no
AMNH:Birds:637450	torotoro	tentelare	Aru Islands, WP	toepad	1896	hyRAD	yes	yes	no	no	no	no
AMNH:Birds:637464	torotoro	tentelare	Aru Islands, WP	toepad	1900	hyRAD	yes	yes	no	no	no	no
AMNH:Birds:637464	torotoro	ochracea	Normanby Island, PNG	toepad	1934	hyRAD	yes	yes	no	no	no	no
CAS:Birds:7131	torotoro	pseuestes	Gulf Province, PNG	muscle	2002	hyRAD	yes	yes	no	no	no	no
KU:Birds:5215	torotoro	pseuestes	Gulf Province, PNG	muscle	2003	hyRAD	yes	yes	no	no	no	no
KU:Birds:5464	torotoro	pseuestes	Gulf Province, PNG	muscle	2003	hyRAD	yes	yes	no	no	no	no
KU:Birds:626	torotoro	meeki	Varirata National Park, PNG	muscle	2011	hyRAD	yes	yes	no	no	no	no
KU:Birds:6927	torotoro	meeki	Mt. Suckling, PNG	muscle	2011	hyRAD	yes	yes	no	no	no	no
NHMUK:Birds:1911.12.20.822	torotoro	pseuestes	Satakwa River, WP	toepad	1911	hyRAD	yes	yes	no	no	no	no
NHMUK:Birds:1911.12.20.823	torotoro	pseuestes	Mimika River, WP	toepad	1913	hyRAD	yes	yes	no	no	no	no

AMNH:Birds:301861	megarhyncha	wellsi	Weylendgep Kunupi, WP	toepad	1931	WGS	yes	yes	yes	yes	yes	yes
AMNH:Birds:302859	megarhyncha	wellsi	Mt. Derimapa, WP	toepad	1930	WGS	yes	yes	yes	yes	yes	yes
AMNH:Birds:339957	megarhyncha	wellsi	Bernhard Camp, WP	toepad	1939	WGS	yes	yes	yes	yes	yes	yes
AMNH:Birds:808986	megarhyncha	megarhyncha	Okapa, PNG	toepad	1965	WGS	yes	yes	yes	yes	yes	yes
ANWC:Birds:B02192	megarhyncha	megrhyncha	Western Highlands, PNG	toepad	1963	WGS	yes	yes	yes	yes	yes	yes
ANWC:Birds:B04293	megarhyncha	megarhyncha	Morobe, PNG	toepad	1966	WGS	yes	yes	yes	yes	yes	yes
ANWC:Birds:B25307	megarhyncha	megarhyncha	Wagau, PNG	toepad	1973	WGS	yes	yes	yes	yes	yes	yes
ANWC:Birds:B25652	megarhyncha	sellamontis	Huon Peninsula, PNG	toepad	1973	WGS	yes	yes	yes	yes	yes	yes
ANWC:Birds:B26140	megarhyncha	sellamontis	Huon Peninsula, PNG	toepad	1973	WGS	yes	yes	yes	yes	yes	yes
YPM:Birds:91444	megarhyncha	sellamontis	Huon Peninsula, PNG	toepad	1969	WGS	yes	yes	yes	yes	yes	yes
AMNH:Birds:329539	torotoro	ochracea	Fergusson Island, PNG	toepad	1928	WGS	yes	yes	yes	yes	yes	yes
AMNH:Birds:329540	torotoro	ochracea	Fergusson Island, PNG	toepad	1928	WGS	yes	yes	yes	yes	yes	yes
AMNH:Birds:426095	torotoro	flavirostris	Fly River, PNG	toepad	1936	WGS	yes	yes	yes	yes	yes	yes
AMNH:Birds:426096	torotoro	flavirostris	Fly River, PNG	toepad	1936	WGS	yes	yes	yes	yes	yes	yes
AMNH:Birds:426121	torotoro	meeki	Wassi Kussi River, PNG	toepad	1937	WGS	yes	yes	yes	yes	yes	yes
AMNH:Birds:637460	torotoro	tentelare	Aru Islands, WP	toepad	1900	WGS	yes	yes	yes	yes	yes	yes
AMNH:Birds:637471	torotoro	meeki	Simbang, PNG	toepad	1899	WGS	yes	yes	yes	yes	yes	yes
AMNH:Birds:637511	torotoro	flavirostris	Cape York Peninsula, AU	toepad	1913	WGS	yes	yes	yes	yes	yes	yes
ANWC:Birds:B07293	torotoro	torotoro	East Sepik Province, PNG	toepad	1966	WGS	yes	yes	yes	yes	yes	yes
ANWC:Birds:B07499	torotoro	torotoro	East Sepik Province, PNG	toepad	1966	WGS	yes	yes	yes	yes	yes	yes

518 **Table 2.** Demographic model test results.

Model	**Log-likelihood**	**AIC**
SC	-564.062	1140.124
AM	-590.0233	1192.047
SIg	-611.0493	1228.099
IMg	-617.116	1244.232
IM	-631.8897	1273.779
SI	-637.185	1280.37
AMg	-653.5472	1319.094
SCg	-716.0587	1444.117

519

520

521

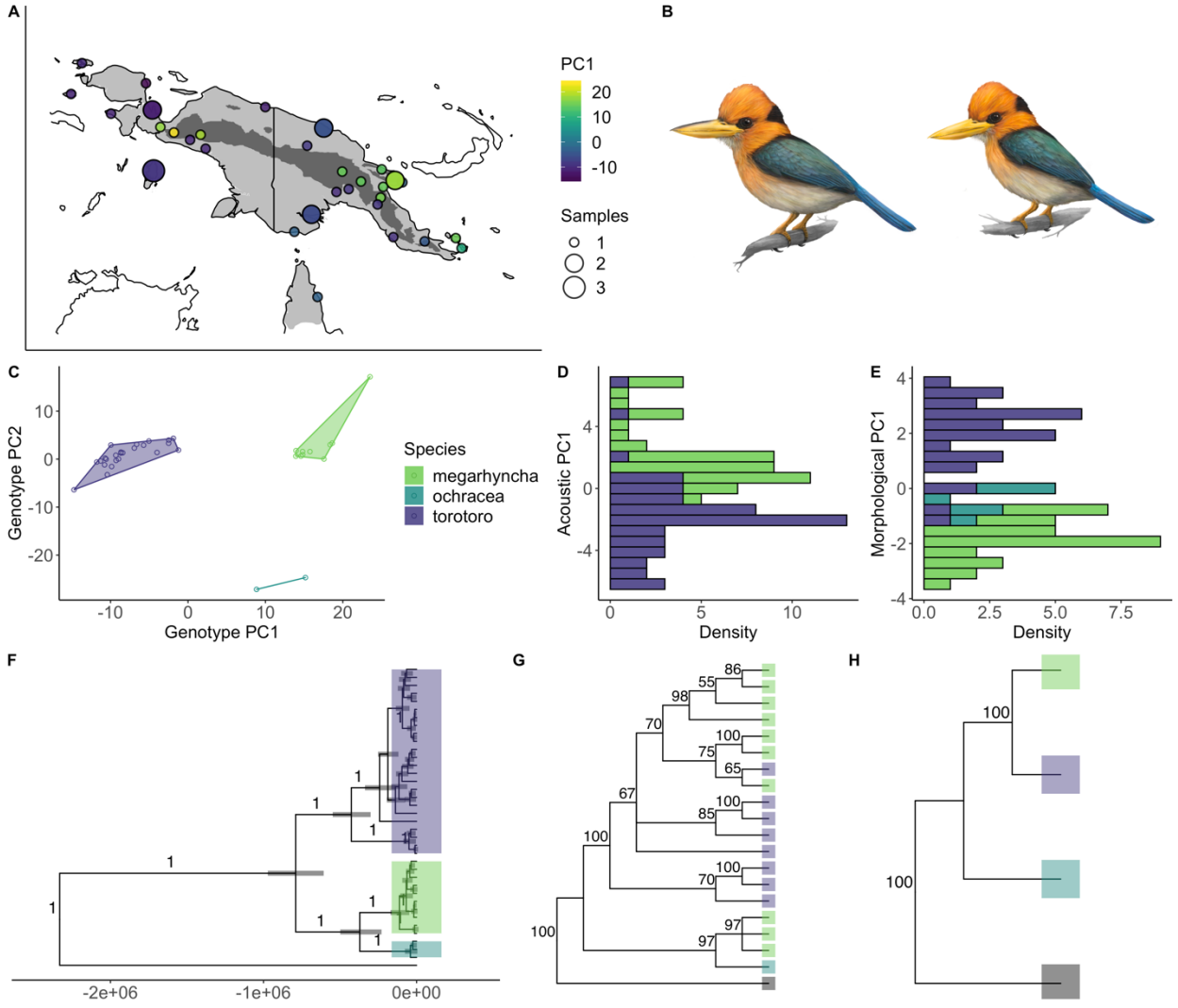

Figure 1. Genomic and phenotypic data provide evidence of assortative mating. A) Sampling localities for *Syma* kingfishers across New Guinea and Australia, color-coded by genotype PC1 and scaled by number of individuals. B) Illustration of *S. megarhyncha* (top) and *S. torotoro* (bottom), by Kevin Epperly. C) Principal component analysis of genotypes, clustered by the best fit *k*-means result (*K*=3) and color-coded by the mean PC1 value for all individuals in a given cluster. D) The first principal component of bioacoustic parameters measured from vocalizations is bimodally distributed by species. E) The first principal component of morphological data is bimodally distributed by species. F) A time-calibrated ND2 phylogeny supports reciprocal monophyly of *S. torotoro* and a clade with *S. megarhyncha* and *S. t. ochracea*. G) SVDquartets nuclear DNA phylogeny. H) SVDquartets species tree, using *k*-means clustering results and mitochondrial DNA clades as taxa.

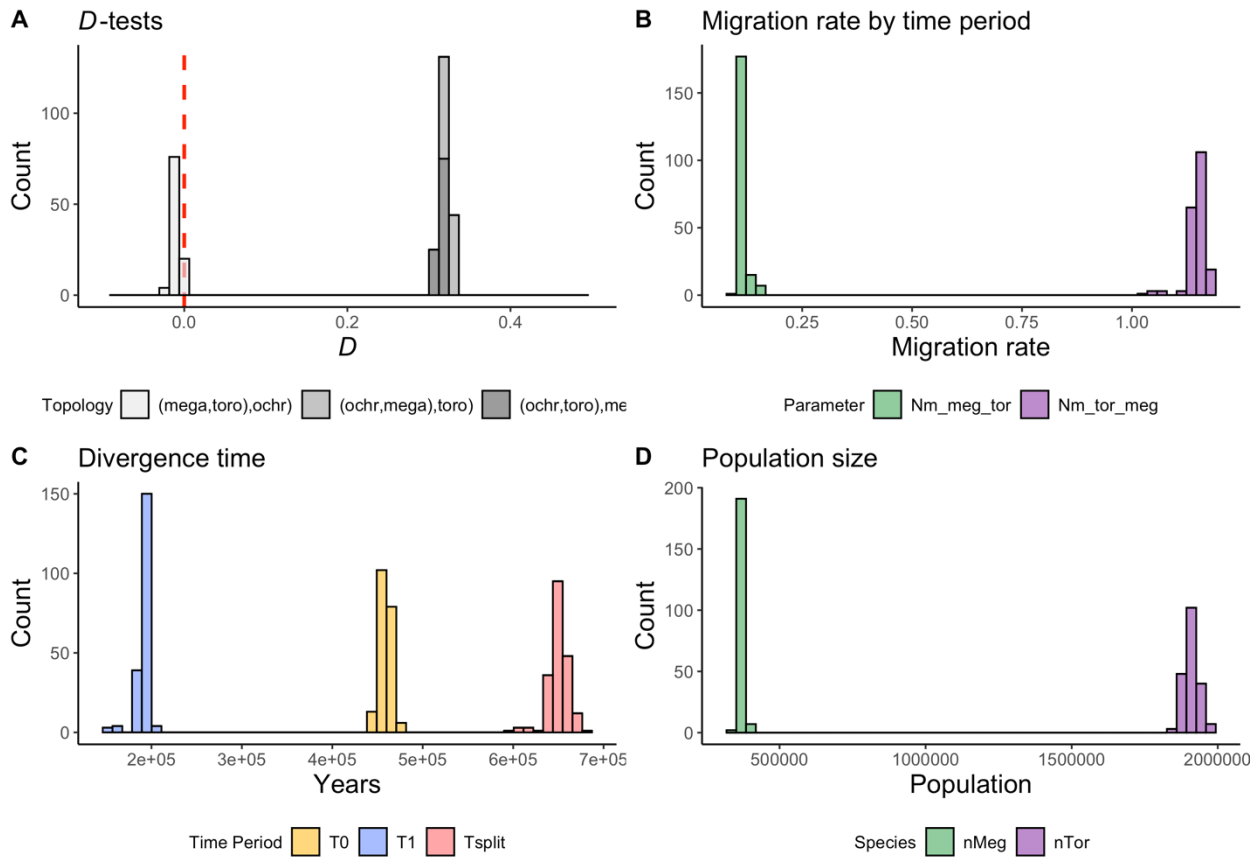

Fig. 2. Evidence for introgression between species. A) Bootstrapped results for D tests for introgression across all three possible species tree topologies. The dashed red line indicates 0, the expectation under incomplete lineage sorting alone. B) Inferred migrants per generation from the best-fit model of secondary contact in *moments*. C) Inferred timing in years of the original divergence event between *S. torotoro* and *S. megarhyncha* ("Tsplit"), the duration of the initial period of isolation ("T0"), and the period of secondary contact ("T1") from *moments*. D) Inferred census population size estimates from *moments.*

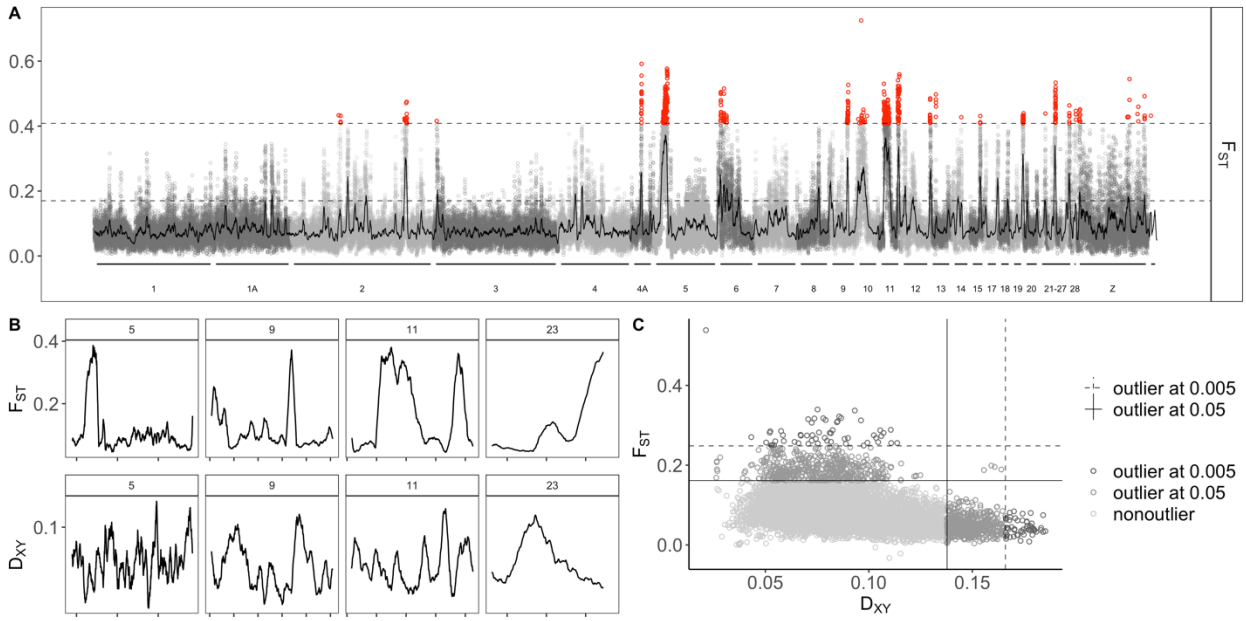

Fig. 3. Heterogeneous genomic divergence. A) Relative divergence (F_{ST}) in 50 kb sliding windows across the genome with 10 kb overlap. Outliers at an arbitrary 0.005 significance level are highlighted in red. B) The genomic landscape of divergence in four chromosomes with strong F_{ST} peaks. C) The correlation between F_{ST} and D_{XY} in the same four chromosomes.

References:

Andersen, M.J., McCullough, J.M., Mauck III, W.M., Smith, B.T., & Moyle, R.G. (2018) A phylogeny of kingfishers reveals an indomalayan origin and elevated rates of diversification on oceanic islands. *Journal of Biogeography*, 45, 269–281.

Andersen, M.J., Shult, H.T., Cibois, A., Thibault, J.C., Filardi, C.E., & Moyle, R.G. (2015). Rapid diversification and secondary sympatry in Australo-Pacific kingfishers (Aves: Alcedinidae: Todiramphus). *Royal Society Open Science*, 2, 140375.

Araya-Salas, M., & Smith-Vidaurre, G. (2017). warbleR: an r package to streamline analysis of animal acoustic signals. *Methods in Ecology and Evolution*, 8, 184–191.

Arteaga, A., Pyron, R.A., Peñafiel, N., Romero-Barreto, P., Culebras, J., Bustamente, L. … Guayasamin, J.M. (2016). Comparative Phylogeography Reveals Cryptic Diversity and Repeated Patterns of Cladogenesis for Amphibians and Reptiles in Northwestern Ecuador. *PLOS ONE*, 11, e0151746.

Bay, R.A., & Ruegg, K. (2017). Genomic islands of divergence or opportunities for introgression? *Proceedings of the Royal Society B: Biological Sciences*, 284, 20162414.

Bouckaert. R., Vaughan, T.G., Barido-Sottani. J., Duchêne. S., Fourment. M., Gavryushkina. A. … Drummond, A.J. (2019). BEAST 2.5: An advanced software platform for Bayesian evolutionary analysis. *PLoS Computational Biology*, 15(4), e1006650.

Beehler, B.M., & Pratt, T.K. (2016). Birds of New Guinea: Distribution, Taxonomy, and Systematics. Princeton, NJ: Princeton University Press.

Beheregaray, L.B., Cooke, G.M., Chao, N.L., & Landguth, E.L. (2015). Ecological speciation in the tropics: insights from comparative genetic studies in Amazonia. *Frontiers in Genetics*, 5.

Burri, R. (2017). Interpreting differentiation landscapes in the light of long-term linked selection. *Evolution Letters*, 1, 118–131.

Cadena, C.D., & Céspedes, L.N. (2019). Origin of elevational replacements in a clade of nearly flightless birds most diversity in tropical mountains accumulates via secondary contact following allopatric speciation. *bioRxiv* 606558.

Cadena, C.D., Kozak, K.H., Gómez, J.P., Parra, J.L., McCain, C.M., Bowie, R.C.K. … Graham, C.H. (2012). Latitude, elevational climatic zonation and speciation in New World vertebrates. *Proceedings of the Royal Society B: Biological Sciences*, 279, 194–201.

Caro, L.M., Caycedo-Rosales, P.C., Bowie, R.C.K., Slabbekoorn, H., & Cadena, C.D. (2013). Ecological speciation along an elevational gradient in a tropical passerine bird? *Journal of Evolutionary Biology*, 26, 357–374.

Chapman, M.A., Hiscock, S.J., & Filatov, D.A. (2013). Genomic divergence during speciation driven by adaptation to altitude. *Molecular Biology and Evolution*, 30, 2553–2567.

Cheviron, Z.A., & Brumfield, R.T. (2009). Migration-selection balance and local adaptation of mitochondrial haplotypes in rufous-collared sparrows (*Zonotrichia capensis*) along an elevational gradient. *Evolution*, 63, 1593–1605.

Chifman, J., & Kubatko, L.K. (2014). Quartet Inference from SNP Data Under the Coalescent Model. *Bioinformatics*, 30, 3317–3314.

Coyne, J.A., & Orr, H.A. (2004). Speciation. Sunderland, MA: Sinauer.

Cruickshank, T.E., & Hahn, M.W. (2014). Reanalysis suggests that genomic islands of speciation are due to reduced diversity, not reduced gene flow. *Molecular Ecology*, 23, 3133–3157.

Danecek, P., Auton, A., Abecasis, G, Albers, C.A., Banks, E., DePristo, M.A. … Durbin, R. (2011) The variant call format and VCFtools. *Bioinformatics*, 27, 2156–2158.

Delcher, A.L., Kasif, S., Fleischmann, R.D., Peterson, J., White, O., & Salzberg, S.L. (1999). Alignment of whole genomes. *Nucleic Acids Research*, 27, 2369–2376.

Derryberry, E.P., Seddon, N., Derryberry, G.E., Claramunt, S., Seeholzer, G.F., Brumfield, R.T., & Tobias, J.A. (2018). Ecological drivers of song evolution in birds: Disentangling the effects of habitat and morphology. *Ecology and Evolution*, 8, 1890–1905.

Diamond, J., Pimm, S.L., Gilpin, M.E., & LeCroy, M. (1989). Rapid Evolution of Character Displacement in Myzomelid Honeyeaters. The American Naturalist, 134, 675–708.

Diamond, J.M. (1972). Avifauna of the Eastern Highlands of New Guinea. Cambridge, MA: Nuttall Ornithological Club.

Doebeli, M., & Dieckmann, U. (2003). Speciation along environmental gradients. *Nature*, 421, 259–264.

Doebeli, M., Dieckmann, U., Metz, J.A.J., & Tautz, D. (2005). What We Have Also Learned: Adaptive Spectiation Is Theoretically Plausible. *Evolution*, 59, 691–695.

DuBay, S.G., & Witt, C.C. (2014). Differential high-altitude adaptation and restricted gene flow across a mid-elevation hybrid zone in Andean tit-tyrant flycatchers. *Molecular Ecology*, 23, 3551–3565.

Dumbacher, J.P., & Fleischer, R.C. (2001). Phylogenetic evidence for colour pattern convergence in toxic pitohuis: Mllerian mimicry in birds? *Proceedings of the Royal Society B: Biological Sciences*, 268, 1971–1976.

Elias, M., Joron, M., Willmott, K., Silvaa-Brandão, K.L., Kaiser, V., Arias, C.F. … Jiggins, C.D. (2009). Out of the Andes: patterns of diversification in clearwing butterflies. *Molecular Ecology*, 18, 1716–1729.

Endler, J.A. (1977). Geographic Variation, Speciation, and Clines. Princeton, NJ: Princeton University Press.

Fitzpatrick, B.M., Fordyce, J.A., & Gavrilets, S. (2008). What, if anything, is sympatric speciation? *Journal of Evolutionary Biology*, 21, 1452–1459.

Freeman, B., & Freeman, A.M.C. (2014). The avifauna of Mt. Karimui, Chimbu Province, Papua New Guinea, including evidence for long-term population dynamics in undisturbed tropical forest. *Bulletin of the British Ornithologists' Club*, 134, 30–51.

Freeman, B.G. (2017). Little evidence for Bergmann's rule body size clines in passerines along tropical elevational gradients. *Journal of Biogeography*, 44, 502–510.

Funk, W.C., Murphy, M.A., Hoke, K.L., Muths, E.L., Amburgey, S.M., Lemmon, E.M., & Lemmon, A.M. (2016). Elevational speciation in action? Restricted gene flow associated with adaptive divergence across an altitudinal gradient. *Journal of Evolutionary Biology*, 29, 241–252.

Gadek, C.R., Newsome, S.D., Beckman, E.J., Chavez, A.N., Galen, S.C., Bautista, E., & Witt, C.C. (2018). Why are tropical mountain passes low for some species? Genetic and stable-isotope tests for differentiation, migration and expansion in elevational generalist songbirds. *Journal of Animal Ecology*, 87, 741–753.

Green, R.E., Krause, J., Briggs, A.W., Maricic, T., Stenzel, U., Kircher, M. … Pääbo, S. (2010). A Draft Sequence of the Neandertal Genome. *Science*, 328, 710–722.

Gregory, P. (2017). Birds of New Guinea. Barcelona, Spain: Lynx Edicions.

Harvey, M.G., Aleixo, A., Ribas, C.C., & Brumfield, R.T. (2017). Habitat Association Predicts Genetic Diversity and Population Divergence in Amazonian Birds. *The American Naturalist*, 190, 631–648.

Hooper, D.M., & Price, T.D. (2017). Chromosomal inversion differences correlate with range overlap in passerine birds. *Nature Ecology & Evolution*, 1, 1526–1534.

Hua, X. (2016) The impact of seasonality on niche breadth, distribution range and species richness: a theoretical exploration of Janzen's hypothesis. *Proceedings of the Royal Society B: Biological Sciences*, 283, 1–8.

Irwin, D.E. (2018). Sex chromosomes and speciation in birds and other ZW systems. *Molecular Ecology,* 27, 3831–3851.

Irwin, D.E., Milá, B., Toews, D.P.L., Brelsford, A., Kenyon, H., Porter, A. … Irwin, J.H. (2018). A comparison of genomic islands of differentiation across three young avian species pairs. *Molecular Ecology*, 27, 4839–4855.

Jankowski, J.E., Ciecka, A.L., Meyer, N.Y., & Rabenold, K.N. (2009). Beta diversity along environmental gradients: implications of habitat specialization in tropical montane landscapes. *Journal of Animal Ecology*, 78, 315–327.

Janzen, D.H. (1967). Why Mountain Passes are Higher in the Tropics. *The American Naturalist*, 101, 233–249.

Jombart, T. (2008). adegenet: a R package for the multivariate analysis of genetic markers. *Bioinformatics*, 24, 1403-1405.

Jónsson, H., Ginolhac, A., Schubert, M., Johnson, P.L.F., & Orlando, L. (2013). mapDamage2.0: fast approximate Bayesian estimates of ancient DNA damage parameters. *Bioinformatics*, 29, 1682–1684.

Jouganous. J., Long, W., Ragsdale, A.P., & Gravel, S. (2017). Inferring the Joint Demographic History of Multiple Populations: Beyond the Diffusion Approximation. *Genetics*, 206, 1549–1567.

Katoh, K., & Standley, D.M. (2013). MAFFT Multiple Sequence Alignment Software Version 7: Improvements in Performance and Usability. *Molecular Biology and Evolution*, 30, 772–780.

Kirkpatrick, M., & Ravigné, V. (2002). Speciation by Natural and Sexual Selection: Models and Experiments. *The American Naturalist*, 159, S22–S35.

Linck, E.B., Hanna, Z.R., Sellas, A., & Dumbacher, J.P. (2017). Evaluating hybridization capture with RAD probes as a tool for museum genomics with historical bird specimens. *Ecology and Evolution*, 7, 4755–4767.

Mallet, J. (2005). Speciation in the 21st century. *Heredity*, 95, 105–109.

Mallet, J. (2008). Hybridization, ecological races and the nature of species: empirical evidence for the ease of speciation. *Philosophical Transactions of the Royal Society B: Biological Sciences*, 363, 2971–2986.

Mayr, E. (1942). Systematics and the Origin of Species, from the Viewpoint of a Zoologist. Cambridge, MA: Harvard University Press.

Miles, A., Ralph, P., Rae, S., & Pisupati, R. (2019). cggh/scikit-allel: v1.2.1 (Version v1.2.1). Zenodo. http://doi.org/10.5281/zenodo.3238280

McCormack, J.E., & Smith, T.B. (2008). Niche expansion leads to small-scale adaptive divergence along an elevation gradient in a medium-sized passerine bird. *Proceedings of the Royal Society B: Biological Sciences*, 275, 2155–2164.

McKenna, A., Hanna, M., Banks, E., Sivachenko, A., Cibulskis, K., Kernytsky, A. … DePristo, M.A. (2010). The Genome Analysis Toolkit: A MapReduce framework for analyzing next-generation DNA sequencing data. *Genome Research*, 20, 1297–1303.

Moyle, R.G., Manthey, J.D., Hosner, P.A., Rahman, M., Lakim, M., & Sheldon, F.H. (2017). A genome-wide assessment of stages of elevational parapatry in Bornean passerine birds reveals no introgression: implications for processes and patterns of speciation. *PeerJ*, 5, e3335.

Nosil, P. (2012). Ecological Speciation. Oxford Series in Ecology and Evolution. Oxford, England, UK: Oxford University Press.

Ortiz, E.M. (2019). vcf2phylip v2.0: convert a VCF matrix into several matrix formats for phylogenetic analysis. (Version v2.0). Zenodo. http://doi.org/10.5281/zenodo.2540861

Osborne, O.G., Batstone, T.E., Hiscock, S.J., & Filatov, D.A. (2013). Rapid Speciation with Gene Flow Following the Formation of Mt. Etna. *Genome Biology and Evolution*, 5, 1704–1715.

Polato, N.R., Gill, B.A., Shah, A.A., Gray, M.A., Casner, K.L., Barthelet, A. … Zamudio, K.R. (2018). Narrow thermal tolerance and low dispersal drive higher speciation in tropical mountains. *Proceedings of the National Academy of Sciences*, 115, 12471–12476.

Portik, D.M., Leaché, A.D., Rivera, D., Barej, M.F., Burger, M., Hirschfield, M. … Fujita, M.K. (2017) Evaluating mechanisms of diversification in a Guineo-Congolian tropical forest frog using demographic model selection. *Molecular Ecology*, 26, 5245–5263.

Pratt, T.K., & Beehler, B.M. (2015). Birds of New Guinea: Second Edition. Princeton, NJ: Princeton University Press.

Price, T. (2008). Speciation in Birds. Greenwood Village, CO: Roberts & Company.

R Core Team. (2018). R: A language and environment for statistical computing.

Rambaut, A., Drummond, A.J., Xie, D., Baele, G., Suchard, M.A. (2018). Posterior Summarization in Bayesian Phylogenetics Using Tracer 1.7. Systematic Biology, 67, 901–904.

Rand, A.L. (1936). Altitudinal variation in New Guinea birds. *American Museum Novitates*.

Ricklefs, R., & Bermingham, E. (2007). The Causes of Evolutionary Radiations in Archipelagoes: Passerine Birds in the Lesser Antilles. *The American Naturalist*, 169, 285–297.

Rundle, H.D., & Nosil, P. (2005). Ecological speciation. Ecology Letters, 8, 336–352.

Sam, K., Koane, B., & Novotny, V. (2014). New avian records along the elevational gradient of Mt. Wilhelm, Papua New Guinea. *Bulletin of the British Ornithologists' Club*, 134, 116–133.

Schluter, D. (2009). Evidence for Ecological Speciation and Its Alternative. Science, 323, 737–741.

Schneider, C.J., Smith, T.B., Larison, B., & Moritz, C. (1999). A test of alternative models of diversification in tropical rainforests: Ecological gradients vs. rainforest refugia. *Proceedings of the National Academy of Sciences*, 96, 13869–13873.

Scrucca, L., Fop, M., Murphy, T.B., & Raftery, A.E. (2016). mclust 5: Clustering, Classification and Density Estimation Using Gaussian Finite Mixture Models. *The R Journal*, 8, 289–317.

Sheldon, K.S., Huey, R.B., Kaspari, M., & Sanders, N.J. (2018). Fifty Years of Mountain Passes: A Perspective on Dan Janzen's Classic Article. *The American Naturalist*, 191, 553–565.

Slabbekoorn, H., & Smith, T.B. (2002). Habitat-Dependent Song Divergence in the Little Greenbul: An Analysis of Environmental Selection Pressures on Acoustic Signals. *Evolution*, 56, 1849–1858.

Smeds, L., Qvarnström, A., & Ellegren, H. (2016). Direct estimate of the rate of germline mutation in a bird. *Genome Research*, 26, 1211–1218.

Smith, B.T., McCormack, J.E., Cuervo, A.M., Hickerson, M.J., Aleixo, A., Cadena, C.D. … Brumfield, R.T. (2014). The drivers of tropical speciation. *Nature*, 515, 406–409.

Smith, J.M. (1966). Sympatric Speciation. *The American Naturalist*, 100, 637–650.

Terborgh, J., & Weske, J.S. (1975). The Role of Competition in the Distribution of Andean Birds. *Ecology*, 56, 562–576.

Toews, D.P.L., & Brelsford, A. (2012). The biogeography of mitochondrial and nuclear discordance in animals. *Molecular Ecology*, 21, 3907–3930.

Turesson, G. (1925). The Plant Species in Relation to Habitat and Climate. *Hereditas*, 6, 147–236.

Via, S. (2009). Natural selection in action during speciation. *Proceedings of the National Academy of Sciences*, 106, 9939–9946.

Via, S. (2012). Divergence hitchhiking and the spread of genomic isolation during ecological speciation-with-gene-flow. *Philosophical Transactions of the Royal Society B: Biological Sciences*, 367, 451–460.

Wiersma, P., Muñoz-Garcia, A., Walker, A., & Williams, J.B. (2007). Tropical birds have a slow pace of life. *Proceedings of the National Academy of Sciences*, 104, 9340–9345.

Winger, B.M., & Bates, J.M. (2015). The tempo of trait divergence in geographic isolation: Avian speciation across the Maraon Valley of Peru. *Evolution*, 69, 772–787.

Zhen, Y., Harrigan, R.J., Ruegg, K.C., Anderson, E.C., Ng, T.C., Lao, S. … Smith, T.B. (2017). Genomic divergence across ecological gradients in the Central African rainforest songbird (*Andropadus virens*). *Molecular Ecology*, 26, 4966–4977.